FATIGUE CRACK GROWTH OF BIFURCATED CRACKS

Marco Antonio Meggiolaro, meggi@puc-rio.br
Antonio Carlos de Oliveira Miranda, amiranda@tecgraf.puc-rio.br
Jaime Tupiassú Pinho de Castro, jtcastro@puc-rio.br
Luiz Fernando Martha, lfm@tecgraf.puc-rio.br
Pontifical Catholic University of Rio de Janeiro, R. Marquês de S. Vicente 225, Rio de Janeiro, RJ, 22541-900, Brazil

Abstract. *Crack bifurcation is a mechanism that can quantitatively explain fatigue crack growth (FCG) retardation effects even in the absence of plasticity induced crack closure. Empirical equations are proposed to calculate the process zone size and stress intensity factors (SIF) along the curved crack branches, based on extensive FE calculations. The equations are a function of the bifurcation angle 2θ, ratio between the branch sizes c_0/b_0, and material crack growth exponent m. In this work, the increase in fatigue life associated with bifurcated cracks under near-threshold conditions is studied. The Levenberg-Marquardt algorithm is used to best fit non-linear equations to the FE results. The results show a competition between the effects of bifurcation and other retardation mechanisms under near-threshold conditions. The presented fatigue life calculation methodology can be used to predict the propagation behavior of bifurcated cracks in an arbitrary structure.*

Keywords*: Fatigue life prediction, bifurcated cracks, crack retardation, mixed mode modeling, finite elements*

1. INTRODUCTION

Fatigue cracks prefer to grow under mode I conditions, changing their path if necessary when loaded under mixed-mode conditions to maintain their sequential increments perpendicular to the maximum normal stress near their tip. However, they can significantly deviate from their usual growth plane due to overloads, sudden changes in the stress field, micro structural characteristics such as grain boundaries and interfaces, or environmental effects, generating crack kinking *or* branching (Lankford and Davidson, 1981; Meggiolaro et al, 2005; Miranda et al, 2005). And a fatigue crack deviated from its usual mode I plane propagates under mixed-mode near-tip conditions even if the far-field stress is purely mode I. Indeed, a pure mode I stress intensity factor (SIF) K_I induces modes I and II SIF k_1 and k_2 near the longer branch of a bifurcated crack and k_1' and k_2' near the shorter one. The equivalent SIF K_b and K_c of the longer and shorter branches, calculated respectively from (k_1, k_2) and (k_1', k_2') using e.g. the $\sigma_{\theta max}$ criterion (Erdogan and Sih, 1963), can be considerably smaller than that of a straight crack with the same projected length, see Fig. 1. Therefore, such branching can retard or even arrest subsequent crack growth (Suresh, 1983).

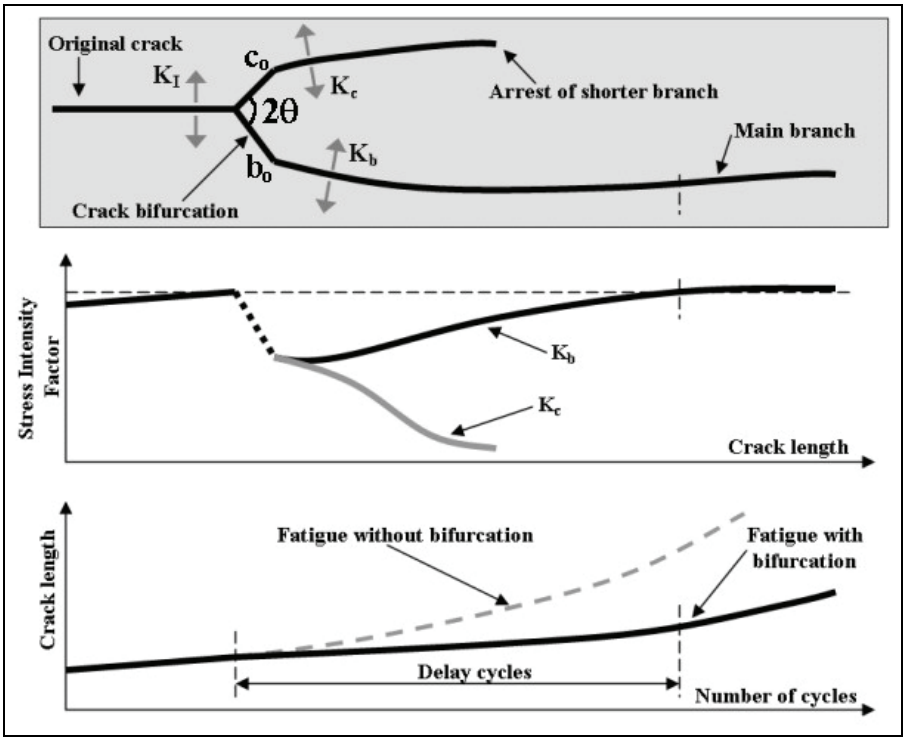

Fig. 1. Typical FCG behavior of bifurcated cracks.

Even very small differences between the crack branch lengths b and c cause the shorter branch c to arrest while the larger one b grows, normally curving its path until reaching approximately its pre-overload SIF and growth direction and rate, see Fig. 1. Hence, although many branches can be developed along the main crack path, only the fastest branches continue to grow, while all others stop due to a shielding effect, a process which also induces crack growth retardation. This typical propagation behavior has been observed in many structural components (Kosec et al, 2002).

There are a few analytical solutions for the SIF of kinked and branched cracks, but it is almost impossible to extend them to describe their complex propagation behavior (Karihaloo, 1982; Seelig and Gross, 1999; Suresh, 1982; Suresh and Shih, 1986). A summary of such SIF solutions is presented in Meggiolaro et al (2005). Therefore, numerical methods such as Finite Elements (FE) and Boundary Elements (BE) are the only practical means to predict the propagation behavior of branched cracks. To predict the generally curved paths of a branched crack and to calculate their associated modes I and II SIF, a specially developed interactive FE program named Quebra2D (2D fracture in Portuguese) is used. This program simulates two-dimensional crack growth based on a FE self-adaptive strategy, using quarter-point crack tip elements and proper crack increment criteria coupled with modern and very efficient automatic remeshing schemes, a fundamental feature to avoid elements with poor aspect ratio, since the size of the larger elements can be 1,000 times bigger than the smaller ones in crack bifurcation calculations. Quebra2D uses an innovative algorithm based in a quadtree procedure to develop local guidelines to generate elements with the best possible shape. The internal nodes are generated simultaneously with the FE, using the quadtree procedure only as a node-spacing function. This approach tends to give a better control over the generated mesh quality and to decrease the amount of heuristic cleaning-up procedures. Moreover, it specifically handles discontinuities inside the domain or on boundary of the model. Finally, to enhance the quality of the shape of the mesh element, an *a posteriori* local mesh improvement procedure is used (Miranda et al, 2003). The calculations are described in the next section.

2. PROPAGATION OF BRANCHED CRACKS

The propagation of branched cracks in a standard C(T) specimen with width $w = 32.0mm$, crack length $a = 14.9mm$, and a very small bifurcation with angle 2θ ranging from 40^o to 168^o, initial longer branch length $b_0 = 10\mu m$ and initial shorter branch lengths ranging from $c_0 = 5\mu m$ to $10\mu m$ is modeled in the Quebra2D program. A fixed crack growth step of $\Delta b = 3\mu m$ (or $1\mu m$ during the first propagation steps) is considered for the propagation of the longer branch b. This growth step is calculated in the direction defined by the $\sigma_{\theta max}$ criterion. Due to the differences in the crack growth rate, a growth step Δc smaller than Δb is expected for the shorter branch. This smaller step is obtained assuming a crack propagation law that models the first two FCG phases,

$$da/dN = A \cdot (\Delta K - \Delta K_{th})^m \tag{1}$$

where A and m are material constants and ΔK_{th} is the propagation threshold. If ΔK_b and ΔK_c are respectively the stress intensity ranges of the longer and shorter branches, then the growth step Δc of the shorter branch c should be

$$\Delta c = \Delta b \cdot \left[(\Delta K_c - \Delta K_{th}) / (\Delta K_b - \Delta K_{th}) \right]^m \tag{2}$$

Interestingly, the ratio between the propagation rates of the two branches is independent of the FCG rule constant A. The exponent m is assumed to be 2.0, 3.0, and 4.0, to reproduce the typical steel exponents measured in practice. Note that a similar expression can be obtained if crack closure effects are considered, even including mean load effects through a function $f(R)$ of the load ratio R, using the effective SIF $\Delta K_{eff} = K_{max} - K_{op}$:

$$\frac{da}{dN} = A \cdot (K_{max} - K_{op})^m \cdot f(R) \Rightarrow \Delta c = \Delta b \cdot \left(\frac{K_{max,c} - K_{op}}{K_{max,b} - K_{op}} \right)^m \tag{3}$$

where $K_{max,b}$ and $K_{max,c}$ are the maximum SIF of the longer and shorter branches respectively, and K_{op} is the crack opening SIF, assumed equal for both branches.

Both the crack path and the associated SIF along each branch are obtained using the Quebra2D program. Several FE calculations were performed for different values of the exponent m, bifurcation angle 2θ, relation c_0/b_0, and SIF, supposing no crack closure no closure effects, $K_{op} = 0$. Closure effects are considered in Miranda et al (2005). Fig. 2 shows the contour plots of the normal stress component in the load direction axis and propagation results for a bifurcated crack with angle $2\theta = 150^o$, obtained from the FE analysis for $c_0/b_0 = 0.91$, $m = 2$ and no closure. In this figure, the deformations are highly amplified to better visualize the crack path. Note that the crack path deviates from the original branch angles, deflecting from $\pm 75^o$ to approximately $\pm 28^o$. In addition, the originally shorter branch arrests after propagating for only about $29\mu m$, while the longer branch returns to the pre-overload growth direction and SIF (even though the subsequent crack growth plane may be offset from the pre-overload one, see Fig. 2).

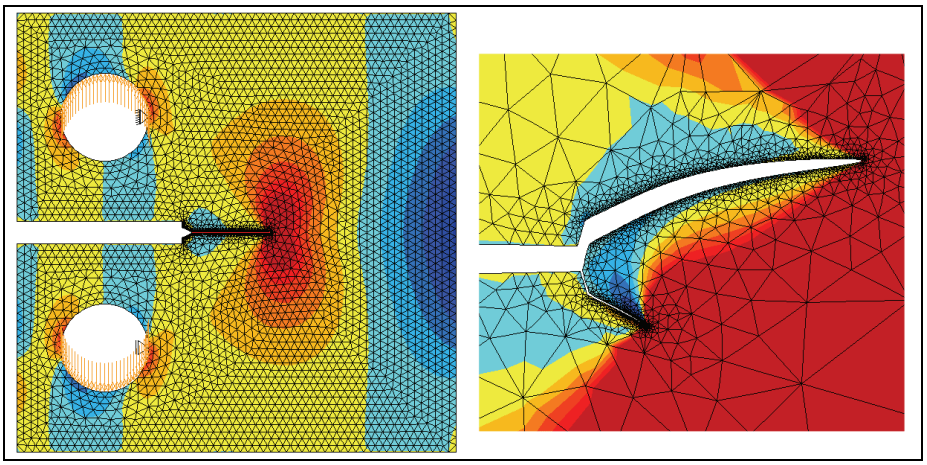

Fig. 2. Propagation simulation of a bifurcated crack on a C(T) specimen (left), and close-up view of the two original $11\mu m$ and $10\mu m$ branches with angle $2\theta = 150^o$ (right).

Figure 3 shows the crack paths predicted from the FE analyses of 4 bifurcated cracks with the same angle $2\theta = 130^o$ and different ratios $c_0/b_0 = \{0.5, 0.8, 0.95, 1\}$, considering $m = 2$ and no closure effects. The dashed lines show the theoretical propagation behavior of a perfectly symmetric bifurcation ($c_0/b_0 = 1$). In this case, the retardation effect would never end because both branches would propagate symmetrically without arresting. Clearly, such idealized behavior is not observed in practice, since the slightest difference between b_0 and c_0 would be sufficient to induce an asymmetrical behavior. Figure 3 also shows that lower c_0/b_0 ratios result in premature arrest of the shorter crack branch, leading to smaller retardation zones. Also, the propagation path of the longer branch is usually restrained to the region within the dashed lines, while the shorter one is "pushed" outside that envelope due to shielding effects.

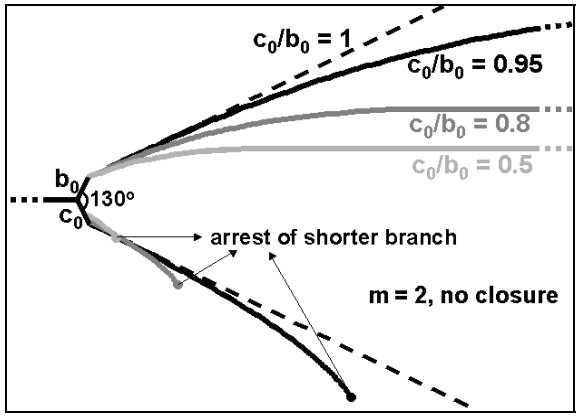

Fig. 3. Bifurcated crack paths for several c_0/b_0 ratios.

The size of the retardation zone can be estimated from the ratio b_f/b_0, where b_f is the value of the length parameter b of the longer branch (measured along the crack path) beyond which the retardation effect ends. The ratio b_f/b_0 is then calculated through FE propagation simulations for all combinations of $c_0/b_0 = \{0.5, 0.8, 0.9, 0.95\}$, $2\theta = \{40^o, 80^o, 130^o, 168^o\}$ and $m = \{2, 3, 4\}$, and fitted by the proposed empirical function:

$$\frac{b_f}{b_0} = \exp\left(\frac{2\theta - 30^o}{56 + 17\cdot(m-2)^{2/3}}\right) \Big/ \left(1 - c_0/b_0\right)^{(12-m)/2\theta} \tag{4}$$

Figure 4 compares the fitted and the FE-obtained data for $m = 3$. Note that a greater symmetry between the branches (as the ratio $c_0/b_0 \rightarrow 1.0$) results in a longer retardation zone, as expected from the delayed arrest of the shorter branch.

The FE-calculated equivalent SIF K_b and K_c of the longer and of the shorter branches are now evaluated along the obtained crack paths. Figure 5 plots the crack retardation factors (defined as the ratios between K_b or K_c and the Mode I SIF K_I of a straight crack) for $2\theta = 130^o$ and $m = 2$, as a function of the normalized length $(b-b_0)/b_0$ of the longer branch. Because of the different crack branch lengths, the SIF at the longer one is much higher than that at the shorter branch. Assuming K_b and K_c to be the crack driving force, it can be seen from Figure 5 that the longer branch reaches its minimum propagation rate right after the bifurcation occurs, returning to its pre-overload rate as the crack tip advances away from the influence of the shorter branch. As seen in the figure, the bifurcation-induced retardation behavior is

misleadingly similar to closure-related effects, even though no closure is present in that case. In addition, as the length difference between both branches increases, it is expected that the propagation rate of the shorter one is reduced until it arrests, after which the larger branch will dominate. Note that even small differences between the branch lengths, such as in the case $c_0/b_0 = 0.95$ shown in Fig. 5, are sufficient to cause subsequent arrest of the shorter branch.

An empirical expression is here proposed to model the SIF K_b of the longer branch during the transition between K_{b0} (the value of K_b immediately after the bifurcation event) and the straight-crack K_I (after the retardation effect ends), valid for $b_0 \le b \le b_f$ and $0.7 < c_0/b_0 < 1$:

$$K_b = K_{b0} + \left(K_I - K_{b0}\right)\cdot\left[\, atan\left(3\frac{b-b_0}{b_f-b_0}\right)\Big/ 1.25\right]^{2c_0/b_0} \tag{5}$$

where b_f is given in Equation (4) and K_{b0} (and K_{c0}) by

$$\frac{K_{b0}}{K_I} = 0.75 + (1-\sin\theta)\cdot\left(1-\frac{c_0}{b_0}\right),\quad \frac{K_{c0}}{K_I} = 0.75 - (1-\sin\theta)\cdot\left(1-\frac{c_0}{b_0}\right) \tag{6}$$

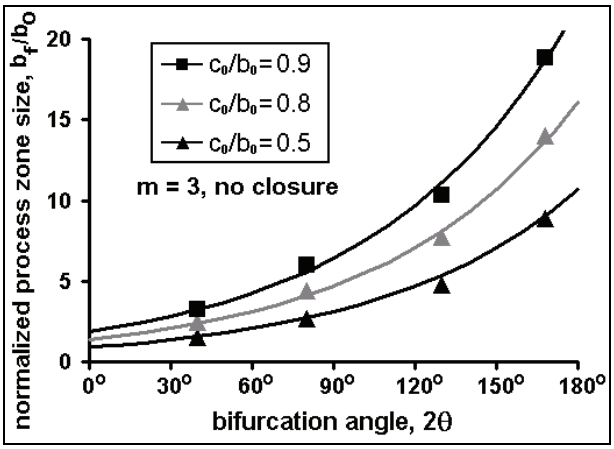

Fig. 4. Normalized process zone size as a function of the bifurcation angle and branch asymmetry c_0/b_0 ($m = 3$).

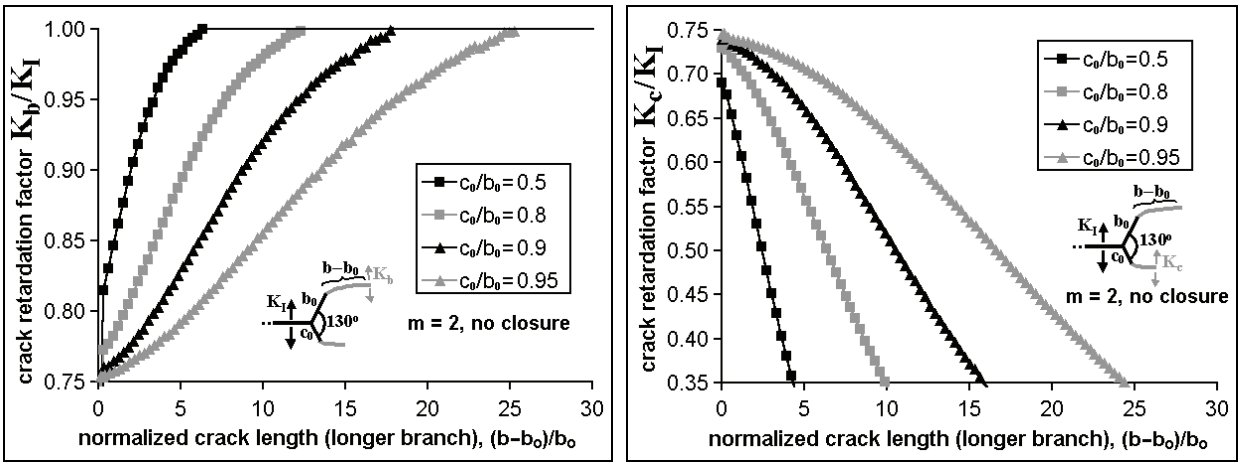

Fig. 5. Normalized equivalent SIF for the (a) longer and (b) shorter branch of a bifurcated crack during its propagation ($2\theta = 130^o$, $m = 2$).

It must be pointed out, however, that the presented FE results and empirical models might have some limitations, because actual bifurcations can be of a size comparable to the scale of the local plasticity (e.g., of the plastic zone size) or microstructural features (e.g., of the grain size). Moreover, possible closure and environmental effects should be considered when comparing the bifurcation model predictions with measured crack growth rates. However, such limitations also apply to all FCG simulations based on SIF driving forces, thus it is no surprise its predictions reproduce reasonably well experimentally measured FCG retardation after a bifurcation, as discussed next.

3. EXPERIMENTAL RESULTS

The predicted bifurcated FCG behavior has been verified on an annealed SAE 4340 steel (C 0.37, Mn 0.56, Si 0.14, Ni 1.53, Cr 0.64, Mo 0.18, S 0.04, P 0.035) ESE(T) specimen with S_Y = 377MPa, S_U = 660MPa, E = 205GPa, and AR = 52.7%. The test has been performed at 30Hz in a 250kN servo-hydraulic testing machine with a baseline stress intensity range ΔK_I = 12.8MPa√m and R = 0.5, following ASTM E 647-99 procedures. The load and the crack-opening displacement (COD) measured by a high speed data acquisition system data has been used to compute the crack closure load using a digitally implemented linearity subtractor output, a circuit developed to precisely measure the opening load (Castro, 1993). The crack branching has been induced by a 100% overload when the crack length was a = 25.55 mm, as described elsewhere (Miranda et al, 2003). Figure 6 shows the retardation effect induced by the bifurcation, leading to approximately 12,600 delay cycles along a process zone of about 0.3mm, and that the R = 0.5 level resulted in no closure effects neither before nor after the overload, because the opening load always remained below the minimum value of the applied load range ΔP. Therefore, it can be concluded that the measured retardation effect cannot be explained by crack closure. In fact, the bifurcation event even reduced the closure level by 25% due to the increased compliance caused by the crack branches. Clearly, retardation effects associated with a reduction in K_{op} would be incompatible with any retardation model based on crack closure. It is implied then that bifurcation is the dominant retardation mechanism.

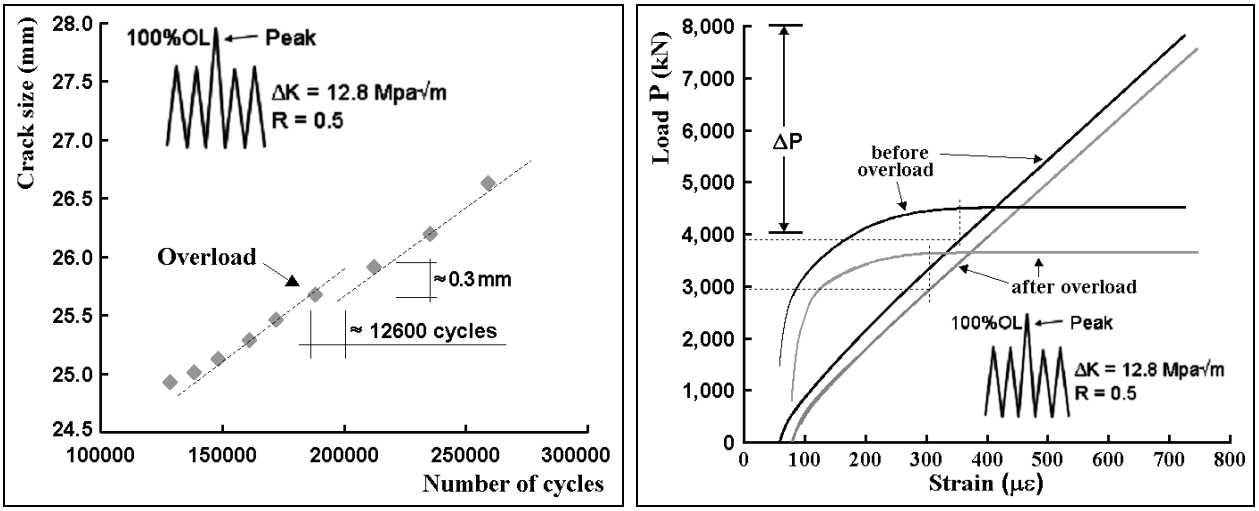

Fig. 6. Fatigue crack growth retardation after a 100 % overload, R = 0.5 (SAE 4340), and opening load measurements, including the output of the linearity subtractor to enhance the nonlinear part of the load versus back face strain ε.

The proposed retardation equations were implemented in a powerful general purpose fatigue life assessment program named ViDa (Meggiolaro and Castro, 2003; Castro et al, 2009), where the estimated number of delay cycles associated with the experimentally obtained bifurcation on the 4340 steel ESE(T) specimen has been calculated. The measured initial branch lengths are approximately b_0 = 20μm and c_0 = 16μm, with a bifurcation angle 2θ = 150°. The material FCG behavior is modeled by equation (1) with $A = 9{\cdot}10^{-11}$ m/cycle, $m = 2.2$, and a threshold $\Delta K_{th} = 3.8$MPa√m, all measured under R = 0.5. Equation (6), is used to obtain the initial ratios K_{b0}/K_I = 0.757 and K_{c0}/K_I = 0.743, leading to ΔK_{b0} = 0.757·ΔK_I = 9.69 and ΔK_{c0} = 0.743·ΔK_I = 9.51MPa√m. Since both ranges are greater than $\Delta K_{th}(R = 0.5) = 3.8$MPa√m, both branches are expected to start propagating, as verified experimentally. Since the measured K_{op} was smaller than the minimum applied SIF (Figure 7), no closure effects need to be considered, therefore the size of the process zone can be estimated directly from Equation (4), which results in b_f = 15.33 × 20μm ≅ 307μm, matching very well the measured process zone size of 0.3mm. The number of cycles in the retardation region is then calculated by integrating the da/dN equation along the longer crack branch, from $b = b_0$ to $b = b_f$. The number of delay cycles n_D can be estimated by:

$$n_D = \int_{b_0}^{b_f} \frac{db}{A(\Delta K_b - \Delta K_{th})^m} - \int_{b_0}^{b_f} \frac{db}{A(\Delta K_I - \Delta K_{th})^m} =$$

$$\int_{20}^{307} \left[\frac{db \times 10^{-6}}{9 \cdot 10^{-11} \left\{ 5.89 + 3.11 \cdot \left[atan\left(3 \frac{b-20}{307-20} \right) \Big/ 1.25 \right]^{1.6} \right\}^{2.2}} - \frac{db \times 10^{-6}}{9 \cdot 10^{-11} (12.8 - 3.8)^{2.2}} \right] = 12{,}024 \text{ cycles} \tag{7}$$

which is very close to the measured 12,600 delay cycles. Therefore, both the process zone size and the number of delay cycles are reasonably well estimated from the proposed equations.

4. CONCLUSIONS

A specialized FE program was used to calculate the propagation path and associated stress intensity factors of bifurcated cracks, which can cause crack retardation or even arrest. A total of 262 crack propagation simulations were obtained from a total of 6,250 FE calculation steps to fit empirical equations to the process zone size and crack retardation factor along the curved crack path. Very small differences between the lengths of the bifurcated branches are sufficient to cause the shorter one to eventually arrest as the longer branch returns to the pre-overload propagation conditions. The proposed equations can be readily used to predict the propagation behavior of branched and kinked cracks in an arbitrary structure, as long as the process zone is small compared to the other characteristic dimensions. From these results, it can be seen that crack bifurcation may provide an alternate explanation for overload-induced crack retardation on structural components, in special to explain load interaction effects under closure-free conditions.

5. REFERENCES

Castro, J.T.P., 1993. "A circuit to measure crack closure", Experimental Techniques v.2, p.23-25.

Castro, J.T.P.; Meggiolaro, M.A. and Miranda, A.C.O., 2009 "Fatigue crack growth predictions based on damage accumulation calculations ahead of the crack tip", Computational Materials Science v.46, p.115-123.

Erdogan, F. and Sih,, G.C., 1963. "On the crack extension in plates under plane loading and transverse shear", Journal of Basic Engineering v. 85, pp.519-527.

Karihaloo, B.L., 1982. "On crack kinking and curving", Mechanics of Materials v.1, pp.189-201.

Kosec, B.; Kovacic, G. and Kosec, L., 2002. "Fatigue cracking of an aircraft wheel", Engineering Failure Analysis v.9, p.603-609.

Lankford, J. and Davidson, D.L., 1981. "The effect of overloads upon fatigue crack tip opening displacement and crack tip opening/closing loads in aluminum alloys", Advances in Fracture Research v.2, pp.899-906, Pergamon Press.

Meggiolaro, M.A., Miranda, A.C.O., Castro, J.T.P. and Martha, L.F., 2005. "Stress intensity factor equations for branched crack growth", Engineering Fracture Mechanics v.72(17), pp.2647-2671.

Meggiolaro, M.A. and Castro, J.T.P., 2003. "On the dominant role of crack closure on fatigue crack growth modeling", International Journal of Fatigue v.25, pp.843-854.

Miranda, A.C.O.; Meggiolaro, M.A.; Castro, J.T.P.; Martha, L.F. and Bittencourt, T.N., 2002. "Fatigue crack propagation under complex loading in arbitrary 2D geometries", ASTM STP 1411 v.4, p.120-146.

Miranda, A.C.O.; Meggiolaro, M.A.; Castro, J.T.P. and Martha, L.F., 2005. "Crack retardation equations for the

Miranda, A.C.O.; Meggiolaro, M.A.; Castro, J.T.P.; Martha, L.F. and Bittencourt, T.N., 2003. "Fatigue life and crack path prediction in generic 2D structural components", Engineering Fracture Mechanics v.70, pp. 1259-1279.

propagation of branched fatigue cracks", International Journal of Fatigue v.27(10-12), pp.1398-1407.

Seelig, T. and Gross, D., 1999. "On the interaction and branching of fast running cracks - a numerical investigation", Journal of the Mechanics and Physics of Solids v.47, pp.935-952.

Suresh, S., 1983. "Crack deflection: implications for the growth of long and short fatigue cracks", Metallurgical Transactions v.14a, pp.2375-85.

Suresh, S., 1983. "Micromechanisms of fatigue crack growth retardation following overloads", Engineering Fracture Mechanics v.18, pp.577-593.

Suresh, S. and Shih, C.F., 1986. "Plastic near-tip fields for branched cracks", International Journal of Fracture v.30, pp.237-259.

7. AKNOWLWDGEMENTS

CNPq has provided research scholarships for the authors.

8. RESPONSIBILITY NOTICE

The authors are the only responsible for the printed material included in this paper.